Effects of land cover transformations on surface microclimate along an urban-rural gradient in Phoenix

Alexander Buyantuyev, Jianguo Wu, and Yun Ouyang
School of Life Sciences, School of Sustainability, Global Institute of Sustainability, Arizona State University, Tempe

CAP LTER
Central Arizona-Phoenix
Long-Term Ecological Research

Integrating Pattern, Process, Scale and Hierarchy
Landscape Ecology and Modeling Laboratory (LEML)
Arizona State University

RESEARCH PROBLEM

Transformations of desert and agricultural lands into urban land covers in Central Arizona alter the surface energy balance and generally increase sensible heat flux to the atmosphere. Locally, highly vegetated and irrigated urban patches increase latent heat exchange and reduce temperatures. The net effect of urbanization is the rural-to-urban differential (the Urban Heat Island (UHI)) characterized by warmer minimum nighttime temperatures within the urban core area. In this study we assess the magnitude of the surface UHI in Phoenix and explore its seasonal and diurnal characteristics using ASTER (Advanced Spaceborne Thermal Emission and Reflection Radiometer) satellite data. We analyzed the effects of land use and cover dynamics on surface microclimate using Landsat satellite data (1985-2005). Key parameters (vegetation cover, soil moisture, surface temperature) were estimated from Landsat images and related to major land cover transitions in the area.

DATA AND METHODS

1) ASTER spectral and thermal images:

- June 2003 and October 2003 land cover maps are produced using Stefanov model applied to the Level 1B data and auxiliary GIS layers. Natural vegetation classes are the result of merging final classifications with the USGS GAP provisional land cover map.
- ASTER normalized difference vegetation index (NDVI), a proxy for vegetative cover, is computed as follows:

$$NDVI = (NIR–RED) / (NIR+RED),$$

where NIR is the near-infrared spectral channel, and RED is the visible red spectral channel of the sensor

2) Landsat TM and ETM+ images

- CAPLTER land cover classifications (1985-2005) used to identify locations land cover changes.
- Surface kinetic temperature grids are produced as part of the atmospheric correction in ATCOR2 module for Erdas Imagine
- Temperature grids are normalized as follows:

$$St^* = (Ts – Ta) / (Ts_{max} – Ta),$$

where St* - scaled surface temperature, Ts – surface temperature, Ta – ambient air temperature, Ts_{max} – temperature of dry, bare soil in in a given image

- NDVI (same as above)
- Normalized Difference Wetness Index (NDWI), a proxy for available surface moisture, is computed as follows:

$$NDWI = (NIR-SWIR) / (NIR+SWIR),$$

where SWIR is the shortwave-near-infrared channel

Table 1. List of satellite images used in the study

Sensor	Spatial resolution: VNIR-SWIR	Spatial resolution: Thermal	Date and time
ASTER	15 (VNIR) 30 m (SWIR)	90 m	06/21/2003 @ 9:41 pm 06/24/2003 @ 11:15 am 10/20/2003 @ 9:35 pm 10/21/2003 @ 11:21 am
Landsat TM	30 m	120 m	07/23/1985 @ 10:33 am 04/24/1987 @ 10:27 am 06/03/1996 @ 10:16 am 06/25/1998 @ 10:42 am 05/11/1999 @ 10:40 am 03/09/2005 @ 10:50 am
Landsat ETM+	30 m	60 m	05/24/2001 @ 10:50 am 05/11/2002 @ 10:52 am

Seasonal and diurnal variations in surface temperature in Phoenix and their relationship with vegetation and microclimate

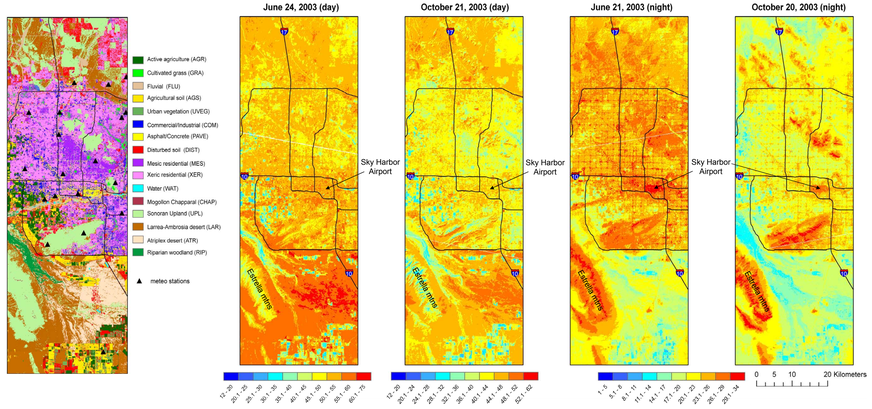

Figure 1. ASTER-derived land use - land cover (June 2003) and surface temperature (in degrees Celsius) maps of Phoenix

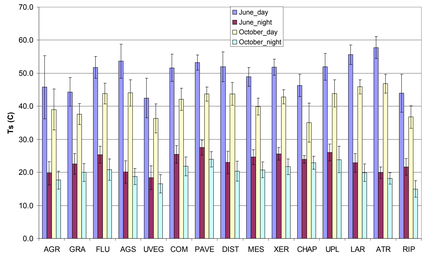

Figure 2. Mean values of surface temperature (in degrees Celsius) associated with land cover categories (see codes in the land cover map legend) shown in Fig. 1. Error bars are ±standard deviation

Table 2. Relationships between surface temperature, NDVI, air temperature, and relative humidity for the group of meteorological stations (n=19) shown in Fig. 1

	Model	R^2	*P*
June-Day			
NDVI	Ts = 68.26 - 32.9 NDVI	0.51	0.0009
Air temperature	Ts = 52.21 + 0.03 Ta	0.00	0.9748
Relative humidity	Ts = 51.27 + 0.13 Rh	0.01	0.6716
June-Night			
NDVI	Ts = 32.71 - 15.31 NDVI	0.18	0.0754
Air temperature	Ts = 9.04 + 0.62 Ta	0.18	0.0813
Relative humidity	Ts = 26.57 - 0.05 Rh	0.01	0.7656
October-Day			
NDVI	Ts = 47.75 - 13.35 NDVI	0.11	0.1639
Air temperature	Ts = 31.21 + 0.35 Ta	0.07	0.2736
Relative humidity	Ts = 43.35 - 0.03 Rh	0.00	0.8988
October-Night			
NDVI	Ts = 25.74 - 8.18 NDVI	0.09	0.2090
Air temperature	Ts = 10.81 + 0.48 Ta	0.35	0.0076
Relative humidity	Ts = 27.32 - 0.15 Rh	0.36	0.0067

June_day

	GRA	UVEG	MES	XER	AGS	COM	PAVE	UPL	LAR	ATR	RIP
AGR	-1.4	-3.3	3.1	6.1	7.9	5.9	7.4	6.2	9.9	12.0	-1.8
GRA		-1.9	4.5	7.5	9.3	7.3	8.8	7.6	11.3	13.4	-0.4
UVEG			6.4	9.4	11.2	9.2	10.7	9.5	13.1	15.3	1.4
MES				3.0	4.8	2.8	4.3	3.1	6.7	8.9	-5.0
XER					1.8	-0.2	1.4	0.1	3.8	6.0	-7.9
AGS						-2.0	-0.5	-1.7	2.0	4.1	-9.7
COM							1.5	0.3	4.0	6.1	-7.7
PAVE								-1.2	2.4	4.6	-9.3
UPL									3.7	5.8	-8.0
LAR										2.2	-11.7
ATR											-13.9

June_night

	GRA	UVEG	MES	XER	AGS	COM	PAVE	UPL	LAR	ATR	RIP
AGR	2.8	-1.4	4.9	5.8	0.4	5.7	7.8	6.3	3.1	0.2	1.9
GRA		-4.2	2.1	3.0	-2.5	2.9	5.0	3.5	0.3	-2.6	-0.9
UVEG			6.2	7.2	1.7	7.1	9.1	7.6	4.5	1.5	3.3
MES				1.0	-4.5	0.8	2.9	1.4	-1.8	-4.7	-3.0
XER					-5.5	-0.1	1.9	0.4	-2.7	-5.7	-3.9
AGS						5.4	7.4	5.9	2.8	-0.2	1.6
COM							2.1	0.6	-2.6	-5.5	-3.8
PAVE								-1.5	-4.7	-7.6	-5.9
UPL									-3.2	-6.1	-4.4
LAR										-2.9	-1.2
ATR											1.7

October_day

	GRA	UVEG	MES	XER	AGS	COM	PAVE	UPL	LAR	ATR	RIP
AGR	-1.4	-2.8	0.9	3.8	5.0	3.0	4.6	4.8	6.8	7.8	-2.3
GRA		-1.3	2.3	5.2	6.4	4.5	6.1	6.2	8.3	9.2	-0.9
UVEG			3.6	6.6	7.7	5.8	7.4	7.6	9.6	10.5	0.5
MES				2.9	4.1	2.2	3.8	3.9	6.0	6.9	-3.2
XER					1.2	-0.8	0.8	1.0	3.0	4.0	-6.1
AGS						-1.9	-0.3	-0.2	1.9	2.8	-7.3
COM							1.6	1.8	3.8	4.7	-5.3
PAVE								0.2	2.2	3.1	-6.9
UPL									2.0	3.0	-7.1
LAR										0.9	-9.1
ATR											-10.1

October_night

	GRA	UVEG	MES	XER	AGS	COM	PAVE	UPL	LAR	ATR	RIP
AGR	2.3	-1.1	3.1	4.1	1.1	4.2	6.3	6.2	2.2	0.5	-2.7
GRA		-3.4	0.7	1.7	-1.2	1.9	4.0	3.9	-0.1	-1.8	-5.0
UVEG			4.2	5.2	2.2	5.3	7.4	7.3	3.3	1.6	-1.6
MES				1.0	-2.0	1.1	3.2	3.1	-0.8	-2.6	-5.8
XER					-2.9	0.1	2.2	2.2	-1.8	-3.5	-6.7
AGS						3.1	5.2	5.1	1.1	-0.6	-3.8
COM							2.1	2.0	-1.9	-3.7	-6.9
PAVE								-0.1	-4.1	-5.8	-9.0
UPL									-4.0	-5.7	-8.9
LAR										-1.7	-4.9
ATR											-3.2

Figure 3. Matrices showing differences in mean surface temperature between pairs of land cover categories. The numbers are derived by subtracting mean surface temperature of land covers shown in the upper row from each of the land cover class shown in the first column. The upper left corner of each matrix contains cross-comparisons of urban/agricultural land covers, while the upper right corner compares anthropogenic with natural land covers. Codes are the same as in Figs. 1 & 2. UHI conditions, when urban land cover classes are warmer than the surrounding desert (excluding riparian), are highlighted.

Land use and land cover changes and associated transformations in vegetation, daytime surface temperature, and soil moisture

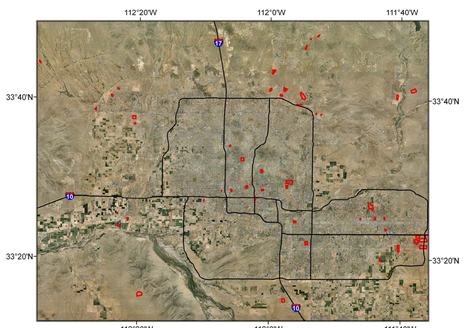

Figure 4. Map of the Phoenix metropolitan region showing locations (red polygons) of selected areas of land cover transitions and controls (no change) during 1985-2005. The backdrop image is the Landiscor aerial photomosaic.

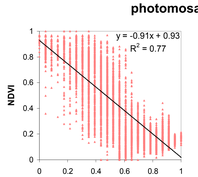

Figure 5. Example of a scatterplot of all pixels within polygons identified in Fig. 4. The year is 1985. Both NDVI and surface temperature (Ts) are normalized.

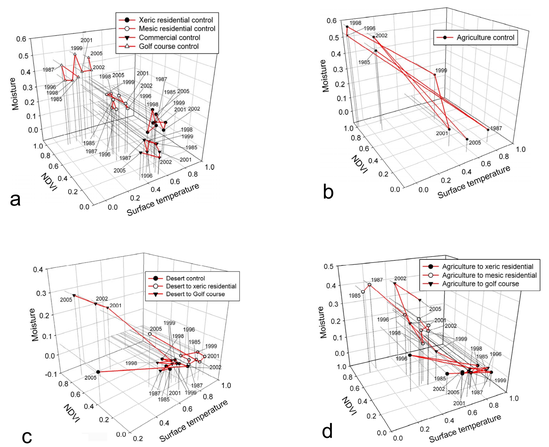

Figure 6. Temporal trajectories of urbanizing pixels (mean of 3 pixels) in the 3-D space of scaled NDVI (vegetation cover) – Surface temperature – Moisture. a) Xeric residential, Mesic residential, Commercial, and Golf course controls (no change); b) agricultural control; c) transitions from desert to urban; d) transitions from agriculture to urban. The approach is borrowed with modifications from (Owen, Carlson and Gillies 1998; Carlson and Arthur 2000)

RESULTS AND CONCLUSIONS

1) Daytime cooling effects of the urbanized landscape (urban heat sink) are generally higher than the nighttime UHI. The highest nighttime gradient develops between *Atriplex*-dominated desert and paved urban surfaces followed by the *Atriplex*-Xeric residential and *Atriplex*-Commerical/Industrial gradients. These patterns are consistent at both seasons but the UHI is greater during the summer (Figs 1,2,3).

2) Riparian woodland is consistently cooler than all natural and anthropogenic (except urban vegetation) land covers. Urban vegetation (parks and other dense vegetation) is the coolest among all land covers at both seasons (Fig. 3).

3) *Atriplex*-dominated desert experiences the highest day-night temperature amplitude at both seasons (Fig. 2).

4) Surface temperature is negatively correlated with NDVI at daytime but insignificantly correlated at night. This pattern is reversed for correlations between air temperature and relative humidity with surface temperature, which are more significant in October (Table 2). These findings will be further investigated by calculating energy balance and heat fluxes with the use of the Grimmond and Oke's Local-Scale Urban Meteorological Parameterization Scheme (LUMPS) model.

5) Pixel trajectories illustrate combined changes in surface microclimate parameters associated with land cover transitions. Control (no change) sites (Fig. 6a) show some variation in surface conditions remaining after normalization or stemming from management practices (i.e. Fig. 6b). Land cover change has variable effects on vegetation cover and surface temperature (Fig. 6c, 6d) which depends on initial conditions and the nature of 'from-to' transformations.

➢Our analysis of diurnal and seasonal variations of surface temperature confirmed the existence of the nighttime surface UHI and the dominance of the daytime heat sink in Phoenix at both the summer and fall seasons. The highest temperature gradient is attributed to differences between paved surfaces and sparsely vegetated *Atriplex*-dominated desert community which has the fastest cooling rate in the absence of incoming solar radiation.

➢Quantification of the effects of urbanization on microclimate conducted via studying interrelationships and temporal changes of key surface parameters (vegetative cover, surface temperature, and soil moisture) derived from satellite data has a potential for developing a predictive statistical model that can help in predicting surface microclimates given different scenarios of urban development.

ACKNOWLEDGEMENTS

The research is supported by the US National Science Foundation under grant No. DEB-0423704 , Central Arizona – Phoenix Long Term Ecological Research (CAPLTER) project. Chris Eisinger's help in obtaining and preparing ASTER data is greatly appreciated.